Journal of Biomolecular Structure and Dynamics

ISSN: (Print) (Online) Journal homepage: https://www.tandfonline.com/loi/tbsd20

Novel oxadiazole-thiadiazole derivatives: synthesis, biological evaluation, and *in silico* studies

Asaf Evrim Evren, Demokrat Nuha, Sam Dawbaa, Abdullah Burak Karaduman, Begüm Nurpelin Sağlik & Leyla Yurttaş

To cite this article: Asaf Evrim Evren, Demokrat Nuha, Sam Dawbaa, Abdullah Burak Karaduman, Begüm Nurpelin Sağlik & Leyla Yurttaş (2023): Novel oxadiazole-thiadiazole derivatives: synthesis, biological evaluation, and *in silico* studies, Journal of Biomolecular Structure and Dynamics, DOI: 10.1080/07391102.2023.2247087

To link to this article: https://doi.org/10.1080/07391102.2023.2247087

JOURNAL OF BIOMOLECULAR STRUCTURE AND DYNAMICS
https://doi.org/10.1080/07391102.2023.2247087

Novel oxadiazole-thiadiazole derivatives: synthesis, biological evaluation, and *in silico* studies

Asaf Evrim Evren[a,b], Demokrat Nuha[a,c], Sam Dawbaa[a,d,e], Abdullah Burak Karaduman[f], Begüm Nurpelin Sağlik[a] and Leyla Yurttaş[a]

[a]Department of Pharmaceutical Chemistry, Faculty of Pharmacy, Anadolu University, Eskişehir, Turkey; [b]Pharmacy Services, Vocational School of Health Services, Bilecik Seyh Edebali University, Bilecik, Turkey; [c]Faculty of Pharmacy, University for Business and Technology, Prishtina, Kosovo; [d]Department of Doctor of Pharmacy (PharmD), Faculty of Medical Sciences, Thamar University, Dhamar, Yemen; [e]Department of Pharmacy, Faculty of Medical Sciences, Al-Hikma University, Dhamar, Yemen; [f]Department of Pharmaceutical Toxicology, Faculty of Pharmacy, Anadolu University, Eskişehir, Turkey

Communicated by Ramaswamy H. Sarma

ABSTRACT

In the search for new anticancer agents, we synthesized a new series of thiazole derivatives carried on thiadiazole-oxadiazole hybrid. Final compounds (**5a–5i**) were analyzed *via* ^{1}H NMR, ^{13}C NMR, and HRMS. The pharmacokinetic profile of the targeted compounds was predicted *via in silico* calculations. Their anticancer properties were determined using MTT method against MCF7 and A549 cell lines. Compounds **5a**, **5b** and **5c** were found more active against MCF7 cells than A549 cells while they were not cytotoxic on L929 healthy cells. Generally, it can be summarized that acetamide moiety has a pivotal role in anticancer activity. For further studies, their aromatase inhibitory activity was evaluated. After determination all these features, the binding modes of the active compounds and the stability and relation of the ligand-enzyme complex were investigated using molecular docking and molecular dynamics simulation studies, respectively. *In vitro* and *in silico* studies suggest two important structure-activity relationship (SAR) points that at least one azole ring is essential, and if there is approximately 8.0 ± 0.5 Å distance between the H-bond rich zone of ligand and the heteroaryl ring system of ligand has a major impact on aromatase inhibitory activity. Compounds with small group substitution on thiazole are found potentially may be used for the treatment of anti-breast cancer orally.

Abbreviations: FAK: Focal-adhesion kinase; ER: Endothelin receptor; EGFR: Epidermal growth factor receptor; CYP51A: Aromatase enzyme; MAP: Methionine aminopeptidase; VEGFR: Vascular endothelial growth factor receptor; HD: Histone deacetylase; TLC: Thin layer chromatography; MTT: 3-(4,5-dimethylthiazol-2-yl)-2,5-diphenyl-2H-tetrazolium bromide; MDS: Molecular dynamics simulation

ARTICLE HISTORY
Received 26 May 2023
Accepted 5 August 2023

KEYWORDS
1,3,4-Oxadiazole; 1,3,4-thiadiazole; cytotoxicity; aromatase inhibition; molecular dynamics simulation

Introduction

Cancer has so many variants and it is a relentless disease (Altintop et al., 2014; Kaplancikli et al., 2012; Mamdani et al., 2022;). So, cancer treatments have also very different approaches and are applied depending on the type/subtype, metastasize, and its current stage (Ganesh & Massague, 2021; Riggio et al., 2021; Yersal & Barutca, 2014; Yin et al., 2020). In spite of those diverse approaches such as chemotherapy, radiotherapy, and surgical intervention, human capabilities are still not sufficient to completely eradicate this disease. Because of that, conducted research and development (R&D) studies are classified simply as designing hit molecules (Hoelder et al., 2012; Sun et al., 2021), testing current bioactive compounds and evaluating their activity through different mechanisms of action (Esmeeta et al., 2022; Pan et al., 2008; Subramaniam et al., 2019; Zhong et al., 2021), and finding new pathways of treatment (Harris, 2020; Old & Chen, 1998; Ross et al., 2014). On the other hand, drug resistance is still a significant issue for chemotherapeutics, like cancer drugs, and this becomes a considerable problem day by day (Holohan et al., 2013; Housman et al., 2014; Leary et al., 2018). In many cancer cases, drug resistance development cause losing its treatment effect, but still, it has side effects (Emran et al., 2022; Raguz & Yague, 2008; Vaidya et al., 2022). Additionally, current anticancer agents are not sufficiently selective against cancer cells than healthy cells. Briefly, for cancer patients, there is an urgent need for new agents at least that they have less cytotoxicity on healthy cells. So, extensive efforts to overcome this issue are achieved consistently (Jiang et al., 2016; Ozben, 2006; Wijdeven et al., 2016).

Nitrogen-rich heterocycles such as azoles take part in the structure of many cancer drugs as shown in Figure 1. The illustrated oxadiazole ring in Figure 1 contributes to several biological properties including anxiolytic (Fasplon), antiviral

CONTACT Asaf Evrim Evren asafevrimevren@anadolu.edu.tr Department of Pharmaceutical Chemistry, Faculty of Pharmacy, Anadolu University, Eskişehir, Turkey

Supplemental data for this article can be accessed online at https://doi.org/10.1080/07391102.2023.2247087.

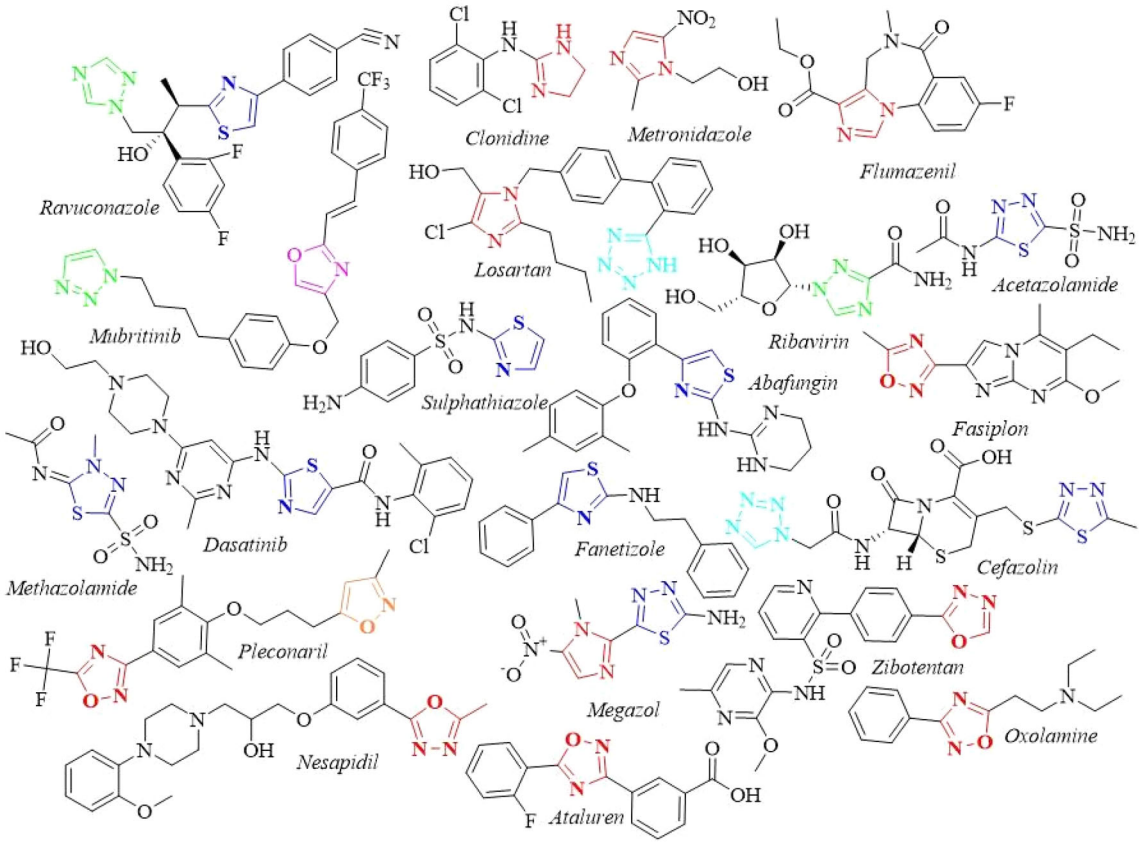

Figure 1. Nitrogen-rich heterocycles drugs. Azoles are colored.

(Pleconaril), antihypertensive (Nesapidil), antiinflammatory (Oxolamine) activity, and efficacy against muscular dystrophy (Ataluren).

The oxadiazole nucleus is also found in anticancer drugs such as Zibotentan and several antitumor agents targeting different proteins such as focal-adhesion kinase (FAK), endothelin receptor (ER), epidermal growth factor receptor (EGFR), vascular endothelial growth factor receptor (VEGFR), methionine aminopeptidase (MAP), histone deacetylase (HD) (Glomb et al., 2018; Matore et al., 2022). Like oxadiazole ring system, thiazole ring has also important various function in pharmacological researches (Altintop et al., 2018; Ertas et al., 2018; Sahin et al., 2018; Venkatesham et al., 2023) and drug development process (Cheng et al., 2021; Liu et al., 2023). The inhibitory effects of oxadiazole-thiadiazole rings on breast cancer (MCF-7) and lung cancer cells (A549) were reported in various studies (Atmaram & Roopan, 2022; Ozdemir et al., 2017; Rashid et al., 2019; Xu et al., 2021; Zhang et al., 2020). For this reason, we shaped the main structure in our study as an oxadiazole-thiadiazole-thiazole rings combination. Furthermore, three azole rings display aromatase enzyme inhibitory activity (Acar Çevik et al., 2023; Avvaru et al., 2021; Çevik et al., 2020).

One of the other important problems is time and money problem during phase 0 (preclinical) studies. However, today, both problems can be reduced using computers. This is an important advantage in preclinic drug development to predict the activity effect of molecules or understand possible binding modes between target proteins and ligands (Evren et al., 2023; Ghanadian et al., 2020; Markovic et al., 2023; Osmaniye et al., 2023; Turan Yucel et al., 2022).

Based on the above information, we aimed to determine the anticancer profiles of the final compounds in this study which include the oxadiazole-thiazole rings combination. After the determination of the active compounds, their possible mechanism of action was evaluated using *in silico* studies.

Materials and methods

Chemistry

All reagents, solvents and other chemicals were obtained either from Merck Chemicals (Merck KGaA, Darmstadt, Germany) or Sigma-Aldrich Chemicals (Sigma-Aldrich Corp., St. Louis, MO, USA). The reactions and possible purities of the compounds were observed by thin layer chromatography (TLC) on silica gel 60 F254 aluminum sheets that were purchased from Merck (Darmstadt, Germany). Melting points of the novel molecules were recorded by MP90 digital melting point apparatus (Mettler Toledo, Ohio, USA). The melting points were presented as uncorrected. Structural analyze of final compounds were investigated using high-resolution mass spectrophotometry (HRMS), ^{1}H-NMR (300 MHz) and ^{13}C-NMR (75 MHz) spectra as in previous studies (Evren et al., 2019; Nuha et al., 2021). Bruker 300 MHz digital FT-NMR spectrometer (Bruker Bioscience, Billerica, MA, USA) in DMSO-d_6 was used for NMR, and LC/MS-IT-TOF system (Shimadzu, Kyoto, Japan) was used for HRMS.

Synthesis of ethyl 2-((5-methyl-1,3,4-thiadiazol-2-yl)thio)acetate (1)

Ethyl 2-bromoacetate (0.044 mol, 4.94 mL) and potassium carbonate (0.055 mol, 7.67 g) were combined with 5-methyl-1,3,4-thiadiazole-2-thiol (0.037 mol, 4.88 g). The mixture was stirred for 1 h in acetone (100 mL). The reaction was monitored using TLC analysis. Upon the completeness of the reaction, the solvent was evaporated and the residue was washed using distilled water and filtered. The dried residue was recrystallized from ethanol.

m. p. 173–175 °C (Yavari et al., 2008), yield 86%.

Synthesis of 2-((5-methyl-1,3,4-thiadiazol-2-yl)thio)acetohydrazide (2)

Ethyl 2-((5-methyl-1,3,4-thiadiazol-2-yl)thio)acetate (**1**) (0.018 mol, 4 g) and hydrazine monohydrate (0.036 mol of 85%, 1.80 mL) were stirred overnight at room temperature in ethanol (80 mL). Following the completeness of the reaction, the mixture was left aside to allow phase separation (formation of a precipitate). The precipitate was obtained *via* filtration and recrystallized from ethanol after drying.

m. p. 173–175 °C (Yavari et al., 2008), yield 81%.

Synthesis of 5-(((5-methyl-1,3,4-thiadiazol-2-yl)thio)-methyl)-1,3,4-oxadiazole-2-thiol (3)

The solution of potassium hydroxide (0.018 mol, 1 g) in ethanol (50 mL) was added to a solution of 2-((5-methyl-1,3,4-thiadiazol-2-yl)thio)acetohydrazide (**2**) (0.015 mol, 3 g) in ethanol (50 mL). After the addition of carbon disulfide (2.7 mL), the mixture was refluxed for 6 h. The reaction mixture was worked up after the completion of the reaction by pouring it into ice water and acidification to pH 5–6 with dilute HCl. The formed precipitate was filtered and dried.

m. p. 173–175 °C (Yavari et al., 2008), yield 71%.

General synthesis of 2-chloro-N-(thiazol-2-yl)acetamide derivatives (4a-4i)

The respective thiazol-2-yl-amine derivative was solved in tetrahydrofuran (THF) with triethylamine as a catalyst and the mixture was stirred in an ice bath for 10 min. A solution of 2-chloroacetyl chloride in THF was added to the mixture dropwise. After adding 2-chloroacetyl chloride, the mixture was stirred at room temperature for 2 h. The reaction was controlled by TLC. The solvent was evaporated after the completion of the reaction, and the solid product was washed with water and filtered. The crude product was recrystallized using ethanol.

General synthesis of 2-((5-(((5-methyl-1,3,4-thiadiazol-2-yl)thio)methyl)-1,3,4-oxadiazol-2-yl)thio)-N-(thiazol-2-yl)acetamide derivatives (5a-5i)

2-Chloro-*N*-(thiazol-2-yl)acetamide derivatives (**4**) (0.001 mol) were mixed with 5-(((5-methyl-1,3,4-thiadiazol-2-yl)thio)-methyl)-1,3,4-oxadiazole-2-thiol (**3**) (0.001 mol, 0.25 g) in acetone 40 mL). Potassium carbonate (0.002 mmol, 0.276 g) was added to the mixture and the mixture was stirred for 2 h at room temperature. TLC was used to monitor the reaction (Mobile phase: EtOAc:PET = 1:3). The acetone was removed when the reaction was completed, and the crude product was washed with water before being recrystallized from ethanol.

2-((5-(((5-Methyl-1,3,4-thiadiazol-2-yl)thio)methyl)-1,3,4-oxadiazol-2-yl)thio)-N-(thiazol-2-yl)acetamide (5a)

m. p. 180–181 °C, yield 84%, ^{1}H-NMR (300 MHz, DMSO-d_6, ppm) δ 2.67 (s, 3H, thiadiazole-$\underline{CH_3}$), 4.35 (s, 2H, acetamide $\underline{CH_2}$), 4.80 (s, 2H, S-$\underline{CH_2}$), 7.25 (d, $J = 3.56$ Hz, 1H, Ar-H), 7.49 (d, $J = 3.56$ Hz, 1H, Ar-H), 12.51 (brs, 1H, $\underline{NH}$). ^{13}C-NMR (75 MHz, DMSO-d_6, ppm) δ 15.71 (thiadiazole-$\underline{CH_3}$), 27.26 (S-$\underline{CH_2}$), 35.80 (acetamide $\underline{CH_2}$), 114.38, 138.23, 162.83, 164.11, 164.89, 165.51, 167.28. HRMS (m/z): $[M+H]^+$ calculated 386.9821; found 386.9808.

2-((5-(((5-Methyl-1,3,4-thiadiazol-2-yl)thio)methyl)-1,3,4-oxadiazol-2-yl)thio)-N-(4-methylthiazol-2-yl)acetamide (5b)

m. p. 184–185 °C, yield 72%, ^{1}H-NMR (300 MHz, DMSO-d_6, ppm) δ 2.34 (s, 3H, thiazole-$\underline{CH_3}$), 2.68 (s, 3H, thiadiazole-$\underline{CH_3}$), 4.33 (s, 2H, acetamide $\underline{CH_2}$), 4.80 (s, 2H, S-$\underline{CH_2}$), 7.16 (s, 1H, Ar-H), 12.33 (brs, 1H, $\underline{NH}$). ^{13}C-NMR (75 MHz, DMSO-d_6, ppm) δ 11.58 (thiazole-$\underline{CH_3}$), 15.74 (thiadiazole-$\underline{CH_3}$), 27.22 (S-$\underline{CH_2}$), 35.76 (acetamide $\underline{CH_2}$), 127.14, 135.39, 162.86, 164.13, 164.88, 165.18, 167.28. HRMS (m/z): $[M+H]^+$ calculated 400.9977; found 400.9960.

Ethyl 2-(2-(2-((5-(((5-methyl-1,3,4-thiadiazol-2-yl)thio)-methyl)-1,3,4-oxadiazol-2-yl)thio)acetamido)thiazol-4-yl)acetate (5c)

m. p. 152–153 °C, yield 68%, ^{1}H-NMR (300 MHz, DMSO-d_6, ppm) δ 1.18 (t, $J = 7.11$ Hz, 3H, O-$\underline{CH_2}$-$\underline{CH_3}$), 2.67 (s, 3H, thiadiazole-$\underline{CH_3}$), 3.69 (s, 2H, thiazole-$\underline{CH_2}$), 4.08 (q, $J = 7.09$ Hz, 2H, O-$\underline{CH_2}$-CH_3), 4.32 (s, 2H, acetamide $\underline{CH_2}$), 4.79 (s, 2H, S-$\underline{CH_2}$), 7.02 (s, 1H, Ar-H), 12.56 (brs, 1H, $\underline{NH}$). ^{13}C-NMR (75 MHz, DMSO-d_6, ppm) δ 14.56 (O-CH_2-$\underline{CH_3}$), 15.71 (thiadiazole-$\underline{CH_3}$), 27.26 (S-$\underline{CH_2}$), 35.78 (thiazole-$\underline{CH_2}$), 37.07 (acetamide $\underline{CH_2}$), 60.80 (O-$\underline{CH_2}$-CH_3), 111.32, 144.27, 157.77, 162.82, 164.07, 164.89, 165.55, 167.28, 170.45. HRMS (m/z): $[M+H]^+$ calculated 473.0189; found 473.0161.

Ethyl 4-methyl-2-(2-((5-(((5-methyl-1,3,4-thiadiazol-2-yl)thio)methyl)-1,3,4-oxadiazol-2-yl)thio)acetamido)thiazole-5-carboxylate (5d)

m. p. 203–204 °C, yield 78%, ^{1}H-NMR (300 MHz, DMSO-d_6, ppm) δ 1.27 (t, $J = 7.08$ Hz, 3H, O-$\underline{CH_2}$-$\underline{CH_3}$), 2.56 (s, 3H, thiazole-$\underline{CH_3}$), 2.68 (s, 3H, thiadiazole-$\underline{CH_3}$), 4.24 (q, $J = 7.10$ Hz, 2H, O-$\underline{CH_2}$-CH_3), 4.37 (s, 2H, acetamide $\underline{CH_2}$), 4.80 (s, 2H, S-$\underline{CH_2}$), 12.90 (brs, 1H, $\underline{NH}$). ^{13}C-NMR (75 MHz, DMSO-d_6, ppm) δ 14.64 (O-CH_2-$\underline{CH_3}$), 15.70 (thiazole-$\underline{CH_3}$), 17.48 (thiadiazole-$\underline{CH_3}$), 27.20 (S-$\underline{CH_2}$), 35.79 (acetamide $\underline{CH_2}$), 61.08 (O-$\underline{CH_2}$-CH_3), 156.75, 159.62, 162.44, 162.85, 163.97, 164.95, 166.56, 167.24. HRMS (m/z): $[M+H]^+$ calculated 473.0189; found 473.0178.

2-((5-(((5-Methyl-1,3,4-thiadiazol-2-yl)thio)methyl)-1,3,4-oxadiazol-2-yl)thio)-N-(4-phenylthiazol-2-yl)acetamide (5e)

m. p. 150–151 °C, yield 86%, ^{1}H-NMR (300 MHz, DMSO-d_6, ppm) δ 2.67 (s, 3H, thiadiazole-CH_3), 4.37 (s, 2H, acetamide CH_2), 4.80 (s, 2H, S-CH_2), 7.34 (d, $J = 7.25$ Hz, 1H, Ar-H), 7.44 (t, $J = 7.69$ Hz, 2H, Ar-H), 7.66 (s, 1H, Ar-H), 7.90 (d, $J = 7.19$ Hz, 2H, Ar-H), 12.68 (brs, 1H, NH). ^{13}C-NMR (75 MHz, DMSO-d_6, ppm) δ 15.73 (thiadiazole-CH_3), 27.27 (S-CH_2), 35.93 (acetamide CH_2), 108.80, 126.13, 128.31, 129.23, 134.67, 149.39, 158.36, 164.15, 164.88, 165.92, 167.26. HRMS (m/z): $[M + H]^+$ calculated 463.0134; found 463.0100.

2-((5-(((5-Methyl-1,3,4-thiadiazol-2-yl)thio)methyl)-1,3,4-oxadiazol-2-yl)thio)-N-(4-(p-tolyl)thiazol-2-yl)acetamide (5f)

m. p. 172–173 °C, yield 81%, ^{1}H-NMR (300 MHz, DMSO-d_6, ppm) δ 2.35 (s, 3H, phenyl-CH_3), 2.67 (s, 3H, thiadiazole-CH_3), 4.36 (s, 2H, acetamide CH_2), 4.80 (s, 2H, S-CH_2), 7.23 (d, $J = 8.06$ Hz, 1H, Ar-H), 7.29 (d, $J = 8.13$ Hz, 1H, Ar-H), 7.58 (s, 1H, Ar-H), 7.77 (s, $J = 7.80$ Hz, 2H, Ar-H) –(metil grup para konusunda olmali, ancak NMR orto konusunda gosteriliyor), 12.67 (brs, 1H, NH). ^{13}C-NMR (75 MHz, DMSO-d_6, ppm) δ 15.70 (thiadiazole-CH_3), 21.33 (phenyl-CH_3), 27.25 (S-CH_2), 35.63 (acetamide CH_2), 108.01, 126.09, 128.32, 129.48, 129.79, 131.96, 137.67, 138.43, 164.94, 165.77, 166.52, 167.27. HRMS (m/z): $[M + H]^+$ calculated 477.0290; found 477.0280.

N-(4-(4-Cyanophenyl)thiazol-2-yl)-2-((5-(((5-methyl-1,3,4-thiadiazol-2-yl)thio)methyl)-1,3,4-oxadiazol-2-yl)thio)acetamide (5 g)

m. p. 158–159 °C, yield 80%, ^{1}H-NMR (300 MHz, DMSO-d_6, ppm) δ 2.68 (s, 3H, thiadiazole-CH_3), 4.24 (s, 2H, acetamide CH_2), 4.80 (s, 2H, S-CH_2), 7.74 (s, 1H, Ar-H), 7.85 (d, $J = 8.52$ Hz, 2H, Ar-H), 8.06 (d, $J = 8.51$ Hz, 2H, Ar-H). ^{13}C-NMR (75 MHz, DMSO-d_6, ppm) δ 15.71 (thiadiazole-CH_3), 27.35 (S-CH_2), 37.81 (acetamide CH_2), 109.76, 111.24, 119.39, 119.54, 126.61, 126.74, 133.12, 133.28, 139.63, 147.07, 164.53, 164.95, 167.30, 167.60. HRMS (m/z): $[M + H]^+$ calculated 488.0086; found 488.0064.

N-(4-(4-Chlorophenyl)thiazol-2-yl)-2-((5-(((5-methyl-1,3,4-thiadiazol-2-yl)thio)methyl)-1,3,4-oxadiazol-2-yl)thio)acetamide (5h)

m. p. 173–174 °C, yield 86%, ^{1}H-NMR (300 MHz, DMSO-d_6, ppm) δ 2.67 (s, 3H, thiadiazole-CH_3), 4.37 (s, 2H, acetamide CH_2), 4.80 (s, 2H, S-CH_2), 7.49 (d, $J = 8.51$ Hz, 2H, Ar-H), 7.72 (s, 1H, Ar-H), 7.91 (d, $J = 8.48$ Hz, 2H, Ar-H), 12.68 (brs, 1H, NH). ^{13}C-NMR (75 MHz, DMSO-d_6, ppm) δ 15.72 (thiadiazole-CH_3), 27.26 (S-CH_2), 35.88 (acetamide CH_2), 109.58, 109.63, 127.85, 129.26, 132.78, 133.51, 148.17, 158.43, 162.82, 164.12, 164.90, 165.96, 167.25. HRMS (m/z): $[M + H]^+$ calculated 496.9744; found 496.9722.

2-((5-(((5-Methyl-1,3,4-thiadiazol-2-yl)thio)methyl)-1,3,4-oxadiazol-2-yl)thio)-N-(5-methyl-4-phenylthiazol-2-yl)acetamide (5i)

m. p. 169–170 °C, yield 79%, ^{1}H-NMR (300 MHz, DMSO-d_6, ppm) δ 2.47 (s, 3H, thiazole-CH_3), 2.67 (s, 3H, thiadiazole-CH_3), 4.34 (s, 2H, acetamide CH_2), 4.80 (s, 2H, S-CH_2), 7.35 (t, $J = 7.39$ Hz, 1H, Ar-H), 7.46 (t, $J = 7.75$ Hz, 2H, Ar-H), 7.64 (d, $J = 7.24$ Hz, 2H, Ar-H), 12.51 (brs, 1H, NH). ^{13}C-NMR (75 MHz, DMSO-d_6, ppm) δ 12.34 (thiazole-CH_3), 15.70 (thiadiazole-CH_3), 27.27 (S-CH_2), 35.76 (acetamide CH_2), 127.80, 128.34, 128.43, 128.57, 128.71, 128.88, 165.50. HRMS (m/z): $[M + H]^+$ calculated 477.0290; found 477.0270.

Biological assays

MTT

The MTT test was used to determine the cytotoxic effects of final compounds (**5a-5i**). The procedure was performed according to our previous studies (Osmaniye et al., 2018; Sağlık et al., 2020). Mouse embryonic fibroblast cell line (NIH/3T3), human lung adenocarcinoma cell line (A549), and human breast cancer cell line (MCF-7) were used in this procedure.

Aromatase inhibition

Bio Vision's Aromatase (CYP19A) Inhibitor Screening Kit (Fluorometric) was used to perform *in vitro* aromatase inhibition experiments (Osmaniye et al., 2018). Dimethyl sulfoxide (DMSO) was used to dissolve the substances, which were then introduced to the test in at least seven different concentrations ranging from 10^{-3} to 10^{-9} M. The results were given as IC_{50} and μM units. The positive control drug was letrozole.

In silico studies

ADME prediction

Some physicochemical properties and pharmacokinetics of the compounds **5a–5i** and reference drug were predicted using the SwissADME web tool (Daina et al., 2017). HBA, H-bond acceptor; HBD, H-bond donor; TPSA, topologic polar surface area (Å^2), Log $P_{o/w,}$ consensus Log $P_{o/w}$ (average of all five predictions), Log S, water solubility; GIA, gastrointestinal absorption; Log K_p, skin permeation (cm/s); RoF (V), Rule of Five (violation number) and SA, synthetic accessibility, was calculated *in silico*.

Molecular docking

Molecular docking studies were performed to define the binding modes of the active compounds in the active regions of the aromatase enzyme X-ray crystal structure (PDB ID: 3EQM) which was retrieved from the Protein Data Bank server (www.pdb.org, accessed April 01, 2021). Schrödinger's Maestro (2020d) interface and its applications (LigPrep module (2020c), Glide module (2020b)) were used for the molecular docking study. Applied procedure was performed same as previously published works (Evren et al., 2022, 2023;

Sahin et al., 2018). Specifically, docking runs were performed in standard precision docking mode (SP).

Molecular dynamics simulation (MDS)

MDS method is a useful technology to predict the time-dependent stability of the systems such as apoproteins, ligand-enzyme or ligand receptor, *etc*. Same methodology routine was performed previously (Dawbaa et al., 2023; Evren et al., 2022; Nuha et al., 2023) by our group. In this study, compound **5a**-protein and compound **5b**-protein systems were investigated through 100 ns. Desmond application of Schrodinger's Maestro (2020a) was used to achieve MDS.

Results and discussion

Chemistry

Compounds **5a–5i** were synthesized according to the detailed methodology and as shown in Scheme 1.

In the first step, ethyl 2-((5-methyl-1,3,4-thiadiazol-2-yl)thio)acetate (**1**) was synthesized from 5-methyl-1,3,4-thiadiazole-2-thiol and ethyl 2-bromoacetate. Then, the obtained product was treated with hydrazine monohydrate to synthesize 2-((5-methyl-1,3,4-thiadiazol-2-yl)thio)acetohydrazide (**2**). Next, the product was reacted with carbon disulfide to synthesize 5-(((5-methyl-1,3,4-thiadiazol-2-yl)thio)methyl)-1,3,4-oxadiazole-2-thiol (**3**). Thiazol-2-ylamine derivatives were acetylated to gain 2-chloro-*N*-(thiazol-2-yl)acetamide derivatives (**4**). In the final step, Compound **3** was treated with compound **4a–4i** using acetone as a solvent to obtain the final products 2-((5-(((5-methyl-1,3,4-thiadiazol-2-yl)thio)-methyl)-1,3,4-oxadiazol-2-yl)thio)-*N*-(thiazol-2-yl)acetamide derivatives (**5**). ^{1}H-NMR, ^{13}C-NMR, and high-resolution mass spectroscopy (HRMS) were used to confirm the structures of the synthesized compounds **5a–5i**. In the ^{1}H-NMR and ^{13}C-NMRspectra, the peaks were seen at their estimated areas. The mass spectra (ESI-MS) of the compounds [$M+1$] peaks were in an agreement with their predicted molecular formula **5a–5i**.

In this study, we synthesized nine new compounds (**5a–5i**), all of which have 2-((5-(((5-methyl-1,3,4-thiadiazol-2-yl)thio)methyl)-1,3,4-oxadiazol-2-yl)thio)-*N*-(thiazol-2-yl)acetamide nucleus in their basic structures. Scheme 1 depicts the steps of the synthesis plan. All of the produced substances were

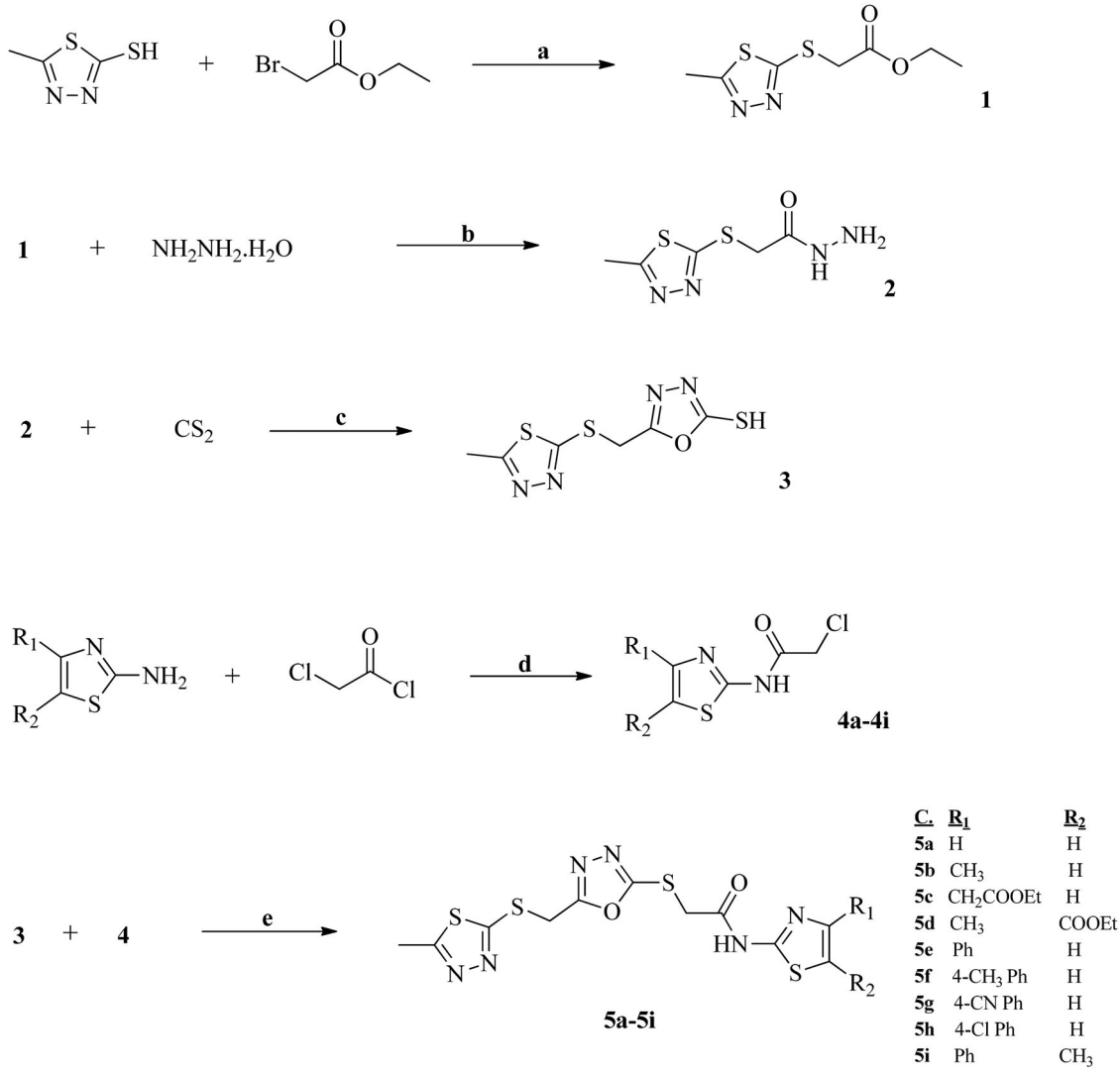

C.	R_1	R_2
5a	H	H
5b	CH_3	H
5c	CH_2COOEt	H
5d	CH_3	COOEt
5e	Ph	H
5f	4-CH_3 Ph	H
5g	4-CN Ph	H
5h	4-Cl Ph	H
5i	Ph	CH_3

Scheme 1. The synthesis diagram of the compounds **5a–5i**. Reagents and conditions: (**a**) K_2CO_3, acetone, r.t., 1 h; (**b**) EtOH, 0–5 °C, then r.t overnight; (**c**) KOH, EtOH, reflux, 6 h (**d**) THF, TEA, 0–5 °C, then r.t 2 h, (**e**) K_2CO_3, acetone, r.t., 2h.

characterized using analytical and spectral data. The ^{1}H-NMR spectra of the compounds showed that thiadiazole-$\underline{CH_3}$ protons were observed at δ 2.67–2.68 ppm as a singlet, acetamide $\underline{CH_2}$ protons were observed at δ 4.24–4.37 ppm as a singlet and S-$\underline{CH_2}$ at δ 4.79–4.80 ppm as a singlet too. A broad singlet peak seen at δ 12.33–12.90 ppm indicated the acetamide N-H proton. The appearance of a pair of singlet, doublets, triplets and/or multiplets at δ 7.16–8.06 ppm was due to the aromatic protons of the aromatic rings. The ^{13}C-NMR spectra of compounds showed signals at δ 15.70–17.48 ppm for thiadiazole-$\underline{CH_3}$ carbon, at δ 27.20–27.35 ppm for S-$\underline{CH_2}$ carbon, at δ 35.76–37.81 ppm for acetamide $\underline{CH_2}$ carbon, at d 108.80–167.30 ppm for aromatic carbon and at δ 165.50–170.45 for carbonyl (C = O) carbon. $M \pm 1$ peaks in LC-MS/MS spectra were in agreed with the calculated molecular weights of the target compounds **5a–5i**.

Biological activity

Cytotoxicity

Final compounds (**5a–5i**) were tested on a healthy mouse embryonic fibroblast cell line NIH/3T3, and two tumor cell lines MCF-7 human breast cancer and A549 human lung cancer cell lines to determine their antiproliferative activity. The half maximal inhibitory concentrations, $IC_{50,}$ were given in μM unit and represented in Table 1.

Compound **5b** exhibited excellent and selective inhibition with an IC_{50} value of 1.033 μM on MCF-7 and 3.914 μM on A549. This is also seen for compound **5e** with an IC_{50} value of 8.322 μM on MCF-7. In addition, compounds **5d, 5g** and **5i** exhibited high and selective antiproliferative effects against MCF-7 cell line with IC_{50} values of 24.820 μM, 37.048 μM and 31.381 μM concentrations, respectively.

Compounds **5a, 5c, 5f** and **5h** were cytotoxic to healthy cells as well as tumor cells. It was observed that the IC_{50} values of these compounds on MCF-7 and A549 cells were higher than the IC_{50} values determined on NIH/3T3, therefore the expected selectivity for anticancer activity was not established.

Aromatase inhibition

The aromatase inhibition effects of compounds **5a–5i** were evaluated, and the half inhibition concentrations (IC_{50}) of the compounds and the standard drug letrozole are presented in Table 2. While the IC_{50} value of letrozole was 0.026 μM, the IC_{50} values of the compounds were found to be in the range of 0.040–2.017 μM. Compound **5a** exhibited the highest aromatase inhibitory activity with an IC_{50} value of 0.040 μM. This compound is followed in the activity order by compound **5c** with an IC_{50} value of 0.062 μM, then compound **5b** with an IC_{50} value of 0.095 μM. These compounds were evaluated as the most active aromatase inhibitor compounds. The IC_{50} values of the remaining compounds were determined at the tested concentrations, but the values found are far from the standard drug, thus, they were inferentially evaluated as not effective.

By evaluating the effect of the thiazole ring's substituents on the activity, compound **5a** (no substituents at C-4 and C-5), is observed as one of the most active compounds. The activity decreases only slightly when the ethyl acetate moiety (**5c**) is brought to the 4th (C-4) position of the thiazole, and also when methyl group (**5b**) is added to the same position. On the other hand, a major decrease in activity was noted in derivatives carrying all 4/5-phenyl thiazole derivatives (**5e–5i**). Other substituents at the 4th and 5th (C-5) positions of the thiazole ring (compounds **5d** and **5i**) also decreased the inhibitory activity on the aromatase enzyme. However, **5d** is still more active than its bulkier analog **5i**. It is concluded that unsubstituted analogs and small-groups substituted thiazole derivatives were more active than bulky groups carrying derivatives. Accordingly, a major impact on activity is observable among the different substituents on the thiazole ring whether they are aliphatic or aromatic or they are small or bulky groups. Occupying either the 4th or both 4th and 5th positions of the thiazole ring also has a significant effect on the activity.

On the other hand, the cytotoxicity investigations on healthy cell line (NIH/3T3) revealed that all of the compounds showed a non-toxic profile on L929 cells at IC_{50} doses against A549 cells, except compounds **5a** and **5c**.

Table 1. IC_{50} values (μM) of the compounds **5a–5i** on NIH/3T3, MCF-7 and A549 cell lines.

	NIH/3T3	MCF-7	A549
5a	46.324 ± 0.694	65.364 ± 1.576	301.159 ± 8.731
5b	68.256 ± 2.900	**1.033 ± 0.006**	**3.914 ± 0.068**
5c	208.453 ± 3.751	446.751 ± 5.924	509.370 ± 8.686
5d	62.952 ± 0.366	24.820 ± 0.970	220.391 ± 6.964
5e	462.664 ± 1.544	**8.322 ± 0.234**	225.708 ± 5.020
5f	55.385 ± 1.174	598.486 ± 6.680	800.574 ± 11.322
5g	61.282 ± 0.958	37.048 ± 0.968	451.504 ± 8.098
5h	58.011 ± 1.092	60.221 ± 0.127	96.370 ± 1.638
5i	37.673 ± 0.583	31.381 ± 0.071	140.284 ± 3.822

Bold value was used to highlight a significantly valuable effect in the activity tables.

Table 2. IC_{50} values (μM) of compounds **5a–5i** and letrozole against aromatase enzymes.

Compounds	Aromatase IC_{50}	Compounds	Aromatase IC_{50}
5a	**0.040 ± 0.002**	**5f**	0.811 ± 0.035
5b	**0.095 ± 0.003**	**5g**	2.017 ± 0.097
5c	**0.062 ± 0.003**	**5h**	1.025 ± 0.040
5d	0.214 ± 0.009	**5i**	1.365 ± 0.055
5e	0.178 ± 0.007	**Letrozole**	0.026 ± 0.001

Table 3. Physicochemical, pharmacokinetic and medicinal chemistry properties of final compounds **5a–5i** by SwissADME.

	Physicochemical Properties				Pharmacokinetics			Medicinal Chemistry	
	HBA	HBD	TPSA	Log $P_{o/w}$	Log S	GIA	Log K_p	RoF (V)	SA
5a	7	1	213.77	2.05	−6.20	Low	−7.18	Yes (0)	3.51
5b	7	1	213.77	2.42	−6.61	Low	−6.98	Yes (0)	3.60
5c	9	1	240.07	2.38	−6.95	Low	−7.57	Yes (0)	3.89
5d	9	1	240.07	2.84	−7.75	Low	−7.02	Yes (0)	3.93
5e	7	1	213.77	3.42	−7.92	Low	−6.47	Yes (0)	3.72
5f	7	1	213.77	3.84	−8.31	Low	−6.29	Yes (0)	3.83
5 g	8	1	237.56	3.25	−8.13	Low	−6.82	Yes (0)	3.78
5h	7	1	213.77	4.04	−8.58	Low	−6.23	Yes (0)	3.69
5i	7	1	213.77	3.78	−8.34	Low	−6.27	Yes (0)	3.85
Ref	4	0	78.29	2.32	−3.70	High	−6.10	Yes (0)	2.13

HBA: H-bond acceptor, **HBD:** H-bond donor, **TPSA:** Topologic polar surface area (Å^2) **Log $P_{o/w}$:** *Consensus* Log $P_{o/w}$ (Average of all five predictions), **Log S:** Water Solubility, **GIA:** Gastrointestinal absorption, **Log K_p:** skin permeation (cm/s), **RoF (V):** Rule of Five (violation number), **SA:** Synthetic accessibility from 1 (very easy) to 10 (very difficult). **Ref:** Reference drug, Letrozole.

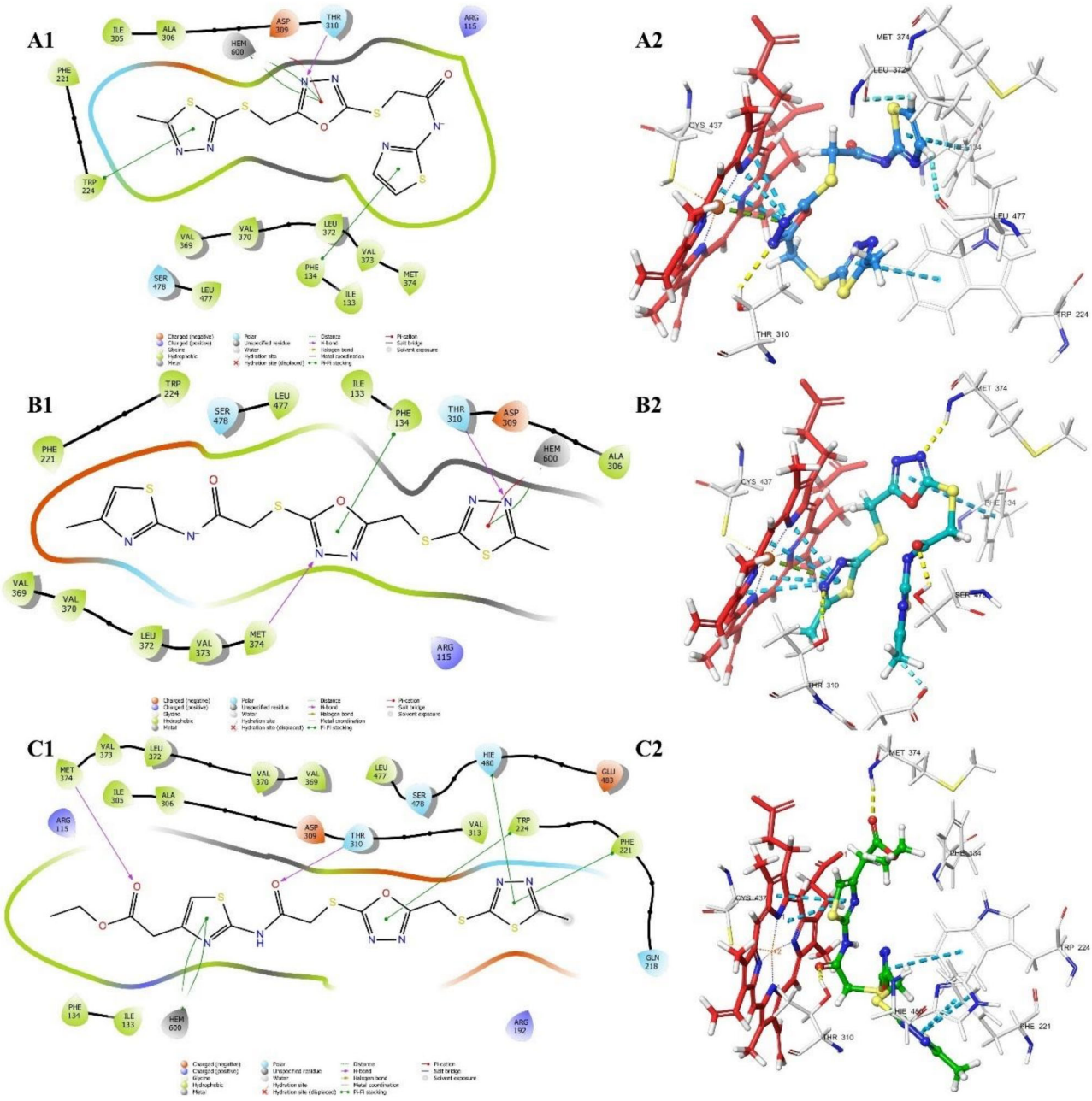

Figure 2. Two- and three-dimensional molecular doking poses of **A)** 5a, **B)** 5b and **C)** 5c. Red carbon-tube model representation is for HEM protein. Only interacted residues are shown for clarity.

Consequently, even though the most potent analog is **5a**, the potential candidate as a drug compound is compound **5b** because of the cytotoxic effect of compound **5a** on healthy cells.

In silico studies

ADME prediction

The key five physicochemical properties were identified using an *in silico* ADME (Absorption, Distribution, Metabolism, and Excretion) investigation of compounds **5a–5i** and letrozole using SwissADME software. Table 3 displays the computational results of the values for HBA, HBD, TPSA, Log P, Log S, Log K, GIA, and other parameters. The target compounds have log P values between 2.05 and 4.04, whereas letrozole has a log P value of 2.32. The number of HBA was 7–9 and HBD was 1 in accordance with Lipinski's 'Rule of 5' (HBD $\leq$ 5, HBA $\leq$ 10). TPSA values were calculated between 213.77 and 240.07 for the compounds while letrozole has a small value of 78.29. Log S which indicates water solubility of the compounds was found quite smaller than letrozole. Besides, log Kp values were predicted between −6.23 and −7.57. However, all compounds adhere to and satisfy the Lipinski rule, with all properties lying within a suitable range, according to their physicochemical properties (Lipinski et al., 1997).

Molecular docking studies

By evaluating all of the experimental studies, the considerable compounds for further *in silico* study were **5a** and **5b**.

Because compounds **5a** and **5c** showed significant *in vitro* aromatase inhibitory activity, we also evaluated their binding mode using the molecular docking method. Results are shown in Figure 2 and interactions are shared in Table 4.

According to molecular docking results, interactions with HEM were *via* π–π stacking, which was observed commonly for them while only compounds **5a** and **5b** interacted directly with Fe atoms. In addition to that, all three interacted with at least one residue at pocket made by ß$_8$ and ß$_9$ strands (ß$_8$–ß$_9$ strands seq. 473–475 and 479–481; ß$_8$–ß$_9$ loop seq. 476–478), while they're also interacted with ß$_3$ strand (seq. 372–376). Also compounds **5a** and **5c** interacted with F α-helix (seq. 210–227) while compounds **5a** and **5b** interacted with Phe134 residue (B'–C loop). Phe134 amino acid approach the substrate from the face of the ligand, while Met374 (ß$_3$ strand) contacts the edge of the ligand and Thr310 approaches the other face of the ligand. Thus, all the above amino acids make an active pocket to bind ligands that results in the stabilization of the enzyme in this way (Ghosh et al., 2010). In this case, the docking studies showed that substituents affect the localization of the thiazole ring into the pocket, but still, they fit in the same space near HEM group (Figure 3).

Table 4. Interaction summary of **5a, 5b** and **5c** at aromatase enzyme active pocket.

Compound	Residue	Interaction number and type
5a	Phe134	1, π-π stacking
	Trp224	1, π-π stacking
	Leu372	1, Ar H-bond
	Leu477	1, Ar H-bond
	HEM	3, π-π stacking
	HEM Fe	1, π-cation
5b	Phe134	1, π-π stacking
	Asp309	1, Ar H-bond
	Thr310	1, H-bond
	Met374	1, H-bond
	Ser478	1, H-bond
	HEM	4, π-π stacking
	HEM Fe	1, π-cation
5c	Phe221	1, π-π stacking
	Thr224	1, π-π stacking
	Thr310	1, H-bond
	Met374	1, H-bond
	Hie480	1, π-π stacking
	HEM	2, π-π stacking

Molecular dynamic simulation studies

Compound **5a** was found to be more active than **5b**, but **5b**'s cytotoxicity on healthy cells resulted favorably. Therefore, we examined the binding modes of both compounds.

Stability plots of compounds **5a** and **5b** are displayed in Figure S29 and Figure S30, respectively. Rg (radius of gyration) peaks did not show drastic changes and those values are between 3.33 and 3.98 Å for **5a**. The same situations were observed for **5b**, 3.29–3.91 Å. On the other hand, RMSD (Root mean square deviation) values were found 1.19–2.23 Å for **5a** and 1.22–1.99 Å for **5b** while fluctuations in both RMSF (root mean square fluctuations) plots of **5a** and **5b** have not showed drastic changes. These three types of plots indicated that both complexes protected the system stability (Dawbaa et al., 2022; Evren et al., 2022, 2023).

The interaction plots of **5a** and **5b** are displayed in Figures 4 and 5 and videos (video1 and video2), respectively.

According to Figures 4 and 5, compound **5a** was interacted with Arg115 (H-bond), Phe134 (π-π stacking), Trp224(π-π stacking), Gln225 (H-bond), and Thr310 (water-mediated H-bond) residues frequently while compound **5b** was with Phe134 (π-π stacking), Gln225 (H-bond), Asp371 (water-mediated H-bond), Leu372 (water-mediated H-bond), and Met374 (H-bond). Interactions with Phe134 residue (B'-C loop) and Gln225 (F helix) are commonly observed. The major impact was caused by Arg115 and Trp224 residues on **5a**'s inhibitory activity while ß3 strand amino acids (like Met374) affected **5b**'s inhibitory activity. However, both MDS results showed that the interactions between thiadiazol-oxadiazole hybrids and aromatase are similar with slight differences.

Structure-activity relationship (SAR)

To simplify the explanation of the SAR, it has been represented in Figure 6 by semi-imaginative visualization

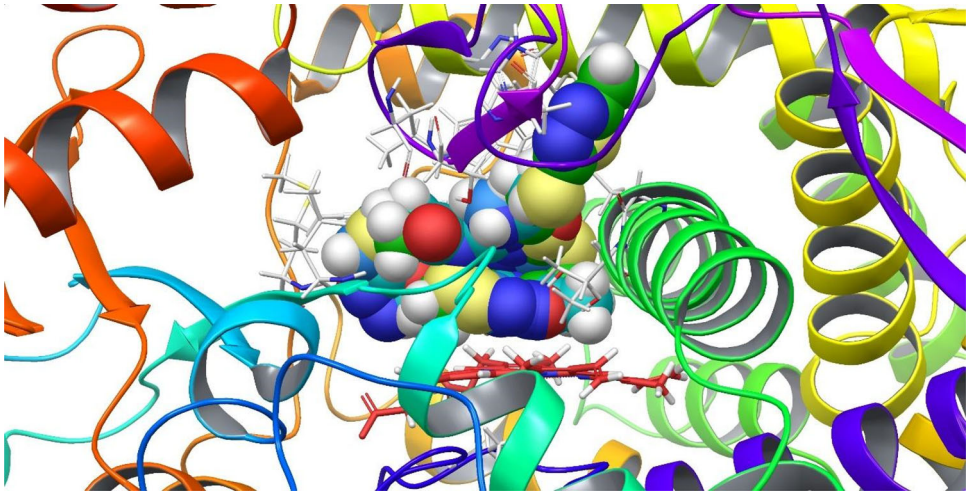

Figure 3. 3D Superimposed **5a**, **5b** and **5c** at aromatase active pocket with ribbon representations. Red carbon-tube model representation is for HEM protein. Only interacted residues are shown for clarity.

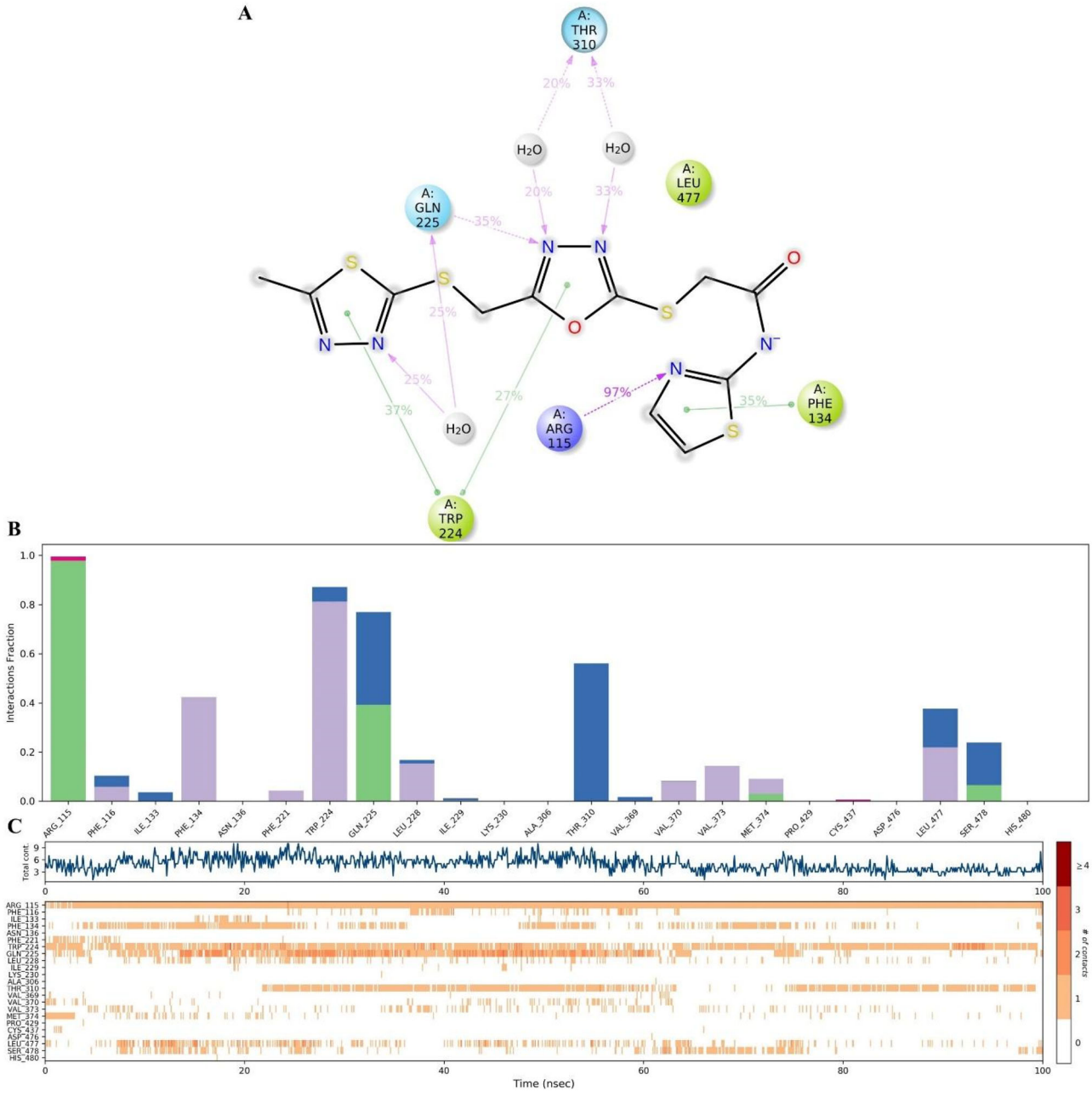

Figure 4. Interaction plots of the MDS results for **5a**-aromatase enzyme complexes. **A**: 2D interaction pose display connection strength (cutoff = 0.2) at the active region **B**: interaction fraction–residue diagram; **C**: total connections–residues–time plot.

according to the *in vitro* and *in silico* studies of how they act in the binding region of the enzyme with typical localizations of those most actives. It's also revealed importantly that the distance between blue pentagon (azol ring system)-iron of HEM was measured in the range of 3.96–6.59 Å during simulation, after 52.8 ns, it was under 5 Å (it was represented purple dashes and its number represent the distance in **video2**). According to literature (Coşkun et al., 2023; Frydenvang et al., 2019), it was in acceptable range for cytochrome enzymes. Moreover, the distance between purple star (enable contacts with ß$_3$ strand and B′–C loop) and red circle (enable contacts with ß$_{8-9}$ or F helix) is calculated between 5.5 and 8.5 Å (Figure S31). Also, in this histogram, the distance was calculated to mean around 6.5 ± 0.5 Å until 52.8 ns while it was around 8.0 ± 0.5 Å from this time to the end of the simulation. As mentioned in *in silico* section, this change allowed for forming H-bond with ß$_{8-9}$ and interacting *via* π–π stacking with the F helix, while π–π stacking with Val370 (K–β$_3$ loop, residue of catalytic cleft) was lost; notwithstanding that, the interactions with Asp371, Leu372 (both also K–β$_3$ loop residues), and Met374 remain continuously. Therefore, for further studies, we offer to obtain significantly better activity that when the new compound has a distance of approximately 8 Å between its H-bond rich area (pink star) and its heteroaryl ring systems (circles, especially red circle) if this part occurs by heteroaryl rings. If it's by carbon chain, this chain should include H-bond donor group(s) to close to ß$_3$ amino acids, but it will result in a loss of connection with Phe134, which is undesirable. The fact that the H-bond rich zone of the ligand is face to F helix, ß3, B′–C loop, and K–ß3

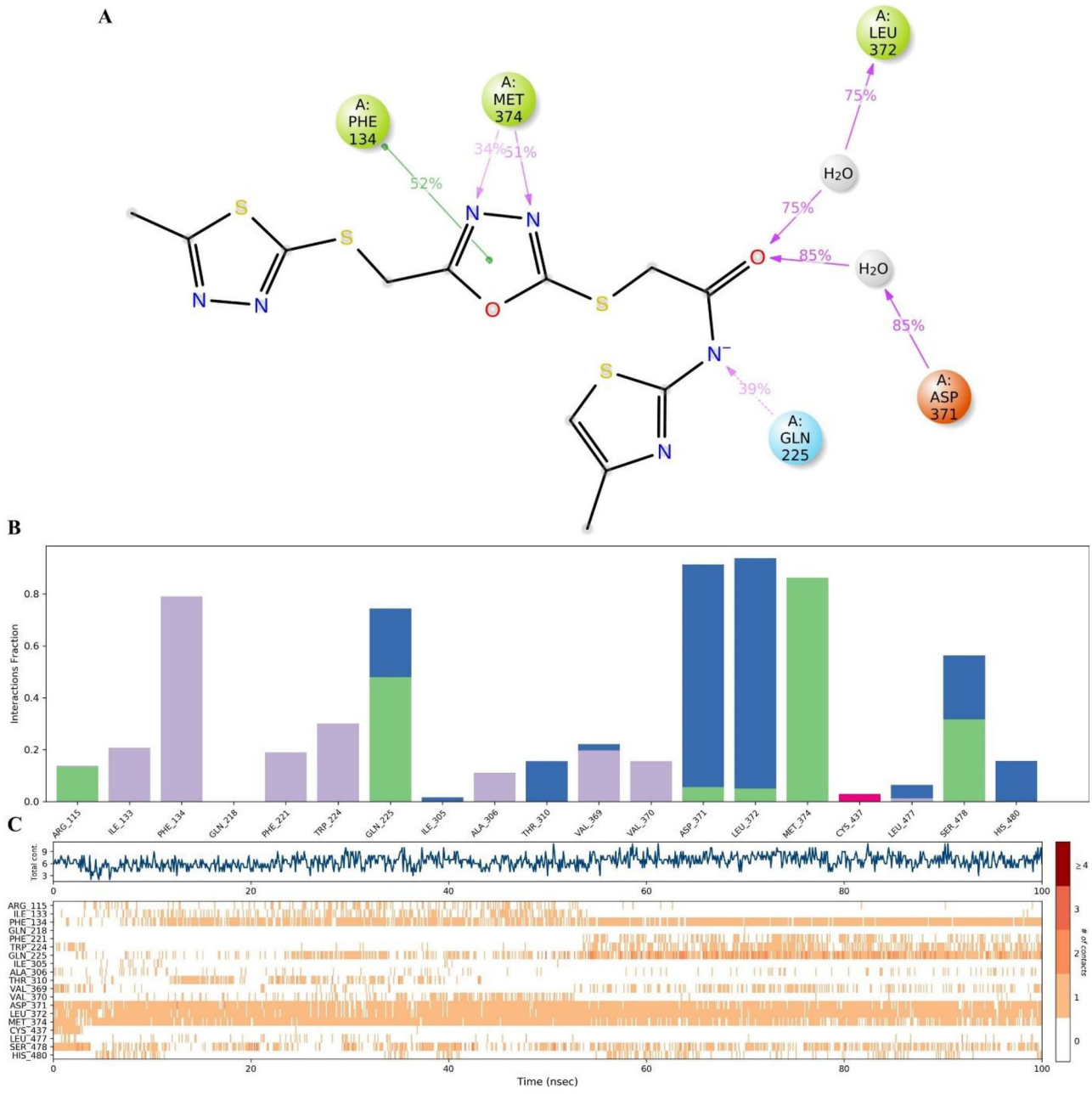

Figure 5. Interaction plots of the MDS results for **5b**-aromatase enzyme complexes. A: 2D interaction pose display connection strength (cutoff = 0.2) at the active region B: interaction fraction–residue diagram; C: total connections–residues–time plot.

loop, therefore aromatic rings seem to be more suitable than carbon chain. On the other hand, the green circle represents the entrance, and the solvent exposure on the enzyme is a major effect here, hence, the equilibrium between hydrophilic and hydrophobic forces of the ligand becomes prominent. Blocking this entrance can be contributed to preventing organic molecules (such as substrates) influx and may induce enzyme stability by interacting with the $ß_9$–$ß_{10}$ loop or F and I helixes. But it's also considered that as reported in one study (Suvannang et al., 2011), despite an inner cavity volume of 1525.92 Å^3, the door of the cavity has only 3.24 Å in diameter. Since bulkier compounds may find it difficult to enter the binding site or not stabilize themself it may need to rotate its side chains to accommodate access to the cavity entrance. In this case, even though three azole rings linked each other with sp^3 atoms in all final molecules, bulky aromatic substitution (**5e–5i**) or 4,5-substitutions (**5d, 5i**) on thiazole ring probably blocked the rotation resulting decrease in the inhibitory effect.

As a result, it's not important which part of the ligand docks into the enzyme because they fit well due to their sp^3 atoms (in this case, acetamide and methyl thiol moieties) as they allow rotation in the active pocket. Contrariwise to that, the essential azole ring (in other words, heterocyclic nitrogen) and the distance between the H-bond rich zone of ligand and heteroaryl ring system of ligand has a major impact on inhibitory activity are very important features, and it is main elicitation from this study. One of the other important elicitations is also acetamide moiety has a pivotal role. The reason for that, it makes a direct H-bond with Gln225 (F helix

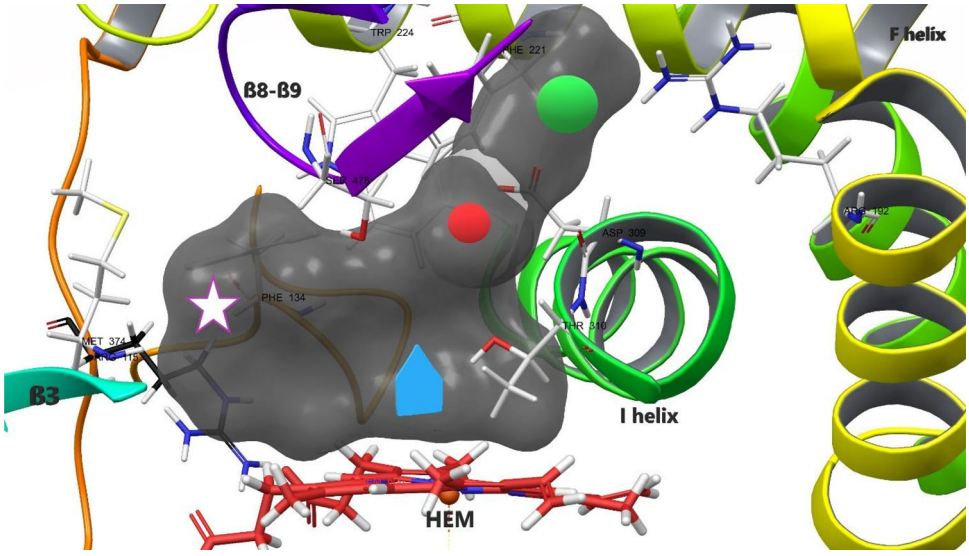

Figure 6. Imaginative visualization represented active compounds and important parts of aromatase enzyme (CYP19A1). circles represents aril groups; pentagon represents essential azole group; purple star represents H-bond acceptors/donors.

amino acid) meanwhile two water-mediated H-bonds with Asp371 and Leu372 (K–$ß_3$ loop amino acids) (see **video-1** and **video-2**). Briefly, the importance of the azole ring system for ligation to the iron of HEM and the distance between interacted parts of the ligand with important parts of protein is explained and proved adding to the literature knowledge.

Conclusions

In this study, nine novel thiadiazole-oxadiazole hybrids, final compounds (**5a–5i**) were synthesized, analyzed, and investigated for their anticancer property against MCF7 breast cancer and A549 lung cancer. After the determination of potential active compounds, their inhibitory effects on aromatase enzymes were evaluated and molecular binding modes were also clarified. Non- or small substitutions on thiazole ring were found more favorable than its bulky analogs against aromatase enzyme, but substitutions reduce cytotoxicity on healthy cells. Therefore, compound **5b** (4-methyl thiazole) is reported as the most potent molecule among thiadiazole-oxadiazole derivatives. Besides that, molecular docking and molecular dynamics studies presented their binding modes and possible behavior of the complex of ligand-enzyme in time versus environmental changes. Also, molecular docking and molecular dynamics studies presented their binding modes and possible behavior of the complex of ligand-enzyme in time versus environmental changes. The key amino acids in enzyme inhibition and in the protection of the stability of complex were evaluated and examined how they affect the protein activity. The remarkable result of this study is one azole ring is essential for inhibition activity as reported in the literature, furthermore, as new information, the significant invention of this study is the 8.0 ± 0.5 Å distance between the H-bond rich zone of ligand and the heteroaryl ring system of ligand has a major impact on aromatase inhibitory activity.

Acknowledgments

The authors present their gratitude to MERLAB and Anadolu University. All analyze data were shared in supplementary file. MDS videos can be watched *via* these links (video1: https://youtu.be/2njF3Udj0eY, Video2: https://youtu.be/cnazMvnPzqc)

Disclosure statement

The author confirms that this article content has no conflict of interest.

Funding

The author(s) reported there is no funding associated with the work featured in this article.

ORCID

Asaf Evrim Evren http://orcid.org/0000-0002-8651-826X

References

Acar Çevik, U., Celik, I., Işık, A., Ahmad, I., Patel, H., Özkay, Y., & Kaplancıklı, Z. A. (2023). Design, synthesis, molecular modeling, DFT, ADME and biological evaluation studies of some new 1,3,4-oxadiazole linked benzimidazoles as anticancer agents and aromatase inhibitors. *Journal of Biomolecular Structure & Dynamics*, *41*(5), 1944–1958. https://doi.org/10.1080/07391102.2022.2025906

Alfaifi, G.H., Farghaly, T.A., Magda, H.A. (2023). Indenyl-thiazole and indenyl-formazan derivatives: Synthesis, anticancer screening studies, molecular-docking, and pharmacokinetic/molin-spiration properties. *PLoS One*, *18* (3), e0274459. https://doi.org/10.1371/journal.pone.0274459

Altintop, M. D., Kaplancikli, Z. A., Ciftci, G. A., & Demirel, R. (2014). Synthesis and biological evaluation of thiazoline derivatives as new antimicrobial and anticancer agents. *European Journal of Medicinal Chemistry*, *74*, 264–277. https://doi.org/10.1016/j.ejmech.2013.12.060

Altintop, M. D., Sever, B., Akalin Ciftci, G., Turan-Zitouni, G., Kaplancikli, Z. A., & Ozdemir, A. (2018). Design, synthesis, in vitro and in silico evaluation of a new series of oxadiazole-based anticancer agents as potential Akt and FAK inhibitors. *European Journal of Medicinal Chemistry*, *155*, 905–924. https://doi.org/10.1016/j.ejmech.2018.06.049

Atmaram, U. A., & Roopan, S. M. (2022). Biological activity of oxadiazole and thiadiazole derivatives. *Applied Microbiology and Biotechnology*, *106*(9–10), 3489–3505. https://doi.org/10.1007/s00253-022-11969-0

Avvaru, S. P., Noolvi, M. N., More, U. A., Chakraborty, S., Dash, A., Aminabhavi, T. M., Narayan, K. P., & Sutariya, V. (2021). Synthesis and anticancer activity of thiadiazole containing thiourea, benzothiazole and imidazo[2,1-b][1,3,4]thiadiazole scaffolds. *Medicinal Chemistry*, *17*(7), 750–765. https://doi.org/10.2174/1573406416666200519085626

Çevik, U. A., Osmaniye, D., Levent, S., Sağlik, B. N., Çavuşoğlu, B. K., Karaduman, A. B., Özkay, Y., & Kaplancikli, Z. A. (2020). Synthesis and biological evaluation of novel 1,3,4-thiadiazole derivatives as possible anticancer agents. *Acta Pharmaceutica (Zagreb, Croatia)*, *70*(4), 499–513. https://doi.org/10.2478/acph-2020-0034

Cheng, Z., Zhang, T., Wang, W., Shen, Q., Hong, Y., Shao, J., Xie, X., Fei, Z., & Dong, X. (2021). D-A-D structured selenadiazolesbenzothiadiazole-based near-infrared dye for enhanced photoacoustic imaging and photothermal cancer therapy. *Chinese Chemical Letters*, *32*(4), 1580–1585. https://doi.org/10.1016/j.cclet.2021.02.017

Coşkun, G., BirgÜL, K., Evren, A. E., Küçükgüzel, ŞG., & Ülgen, M. (2023). In silico studies and in vitro microsomal metabolism of potent MetAP2 inhibitor and in vivo tumor suppressor for prostate cancer: A thioether-triazole hybrid. *Acibadem Universitesi Saglik Bilimleri Dergisi*, *14*(1), 10–23. https://doi.org/10.31067/acusaglik.1210129

Daina, A., Michielin, O., & Zoete, V. (2017). SwissADME: A free web tool to evaluate pharmacokinetics, drug-likeness and medicinal chemistry friendliness of small molecules. *Scientific Reports*, *7*(1), 42717. https://doi.org/10.1038/srep42717

Dawbaa, S., Evren, A. E., Sağlik, B. N., Gundogdu-Karaburun, N., & Karaburun, A. C. (2022). Biological activity evaluation of novel monoamine oxidase inhibitory compounds targeting Parkinson disease. *Future Medicinal Chemistry*, *14*(22), 1663–1679. https://doi.org/10.4155/fmc-2022-0167

Dawbaa, S., Nuha, D., Evren, A. E., CankiliÇ, M. Y., YurttaŞ, L., & Turan, G. (2023). New oxadiazole/triazole derivatives with antimicrobial and antioxidant properties. *Journal of Molecular Structure*. *1282*, 135213. https://doi.org/10.1016/j.molstruc.2023.135213

Emran, T. B., Shahriar, A., Mahmud, A. R., Rahman, T., Abir, M. H., Siddiquee, M. F., Ahmed, H., Rahman, N., Nainu, F., Wahyudin, E., Mitra, S., Dhama, K., Habiballah, M. M., Haque, S., Islam, A., & Hassan, M. M. (2022). Multidrug resistance in cancer: Understanding molecular mechanisms, immunoprevention and therapeutic approaches. *Frontiers in Oncology*, *12*, 891652. https://doi.org/10.3389/fonc.2022.891652

Ertas, M., Sahin, Z., Berk, B., Yurttas, L., Biltekin, S. N., & Demirayak, S. (2018). Pyridine-substituted thiazolylphenol derivatives: Synthesis, modeling studies, aromatase inhibition, and antiproliferative activity evaluation. *Archiv Der Pharmazie*, *351*(3-4), e1700272. https://doi.org/10.1002/ardp.201700272

Esmeeta, A., Adhikary, S., Dharshnaa, V., Swarnamughi, P., Ummul Maqsummiya, Z., Banerjee, A., Pathak, S., & Duttaroy, A. K. (2022). Plant-derived bioactive compounds in colon cancer treatment: An updated review. *Biomedicine & Pharmacotherapy = Biomedecine & Pharmacotherapie*, *153*, 113384. https://doi.org/10.1016/j.biopha.2022.113384

Evren, A. E., Karaduman, A. B., Sağlik, B. N., Özkay, Y., & Yurttaş, L. (2023). Investigation of novel quinoline-thiazole derivatives as antimicrobial agents: In vitro and in silico approaches. *ACS Omega*. *8*(1), 1410–1429. https://doi.org/10.1021/acsomega.2c06871

Evren, A. E., Nuha, D., Dawbaa, S., Sağlık, B. N., & Yurttaş, L. (2022). Synthesis of novel thiazolyl hydrazone derivatives as potent dual monoamine oxidase-aromatase inhibitors. *European Journal of Medicinal Chemistry*, *229*, 114097. https://doi.org/10.1016/j.ejmech.2021.114097

Evren, A. E., Yurttas, L., & Yılmaz-Cankilic, M. (2019). Synthesis of novel N-(naphthalen-1-yl)propanamide derivatives and evaluation their antimicrobial activity. *Phosphorus, Sulfur, and Silicon and the Related Elements*, *195*(2), 158–164. https://doi.org/10.1080/10426507.2019.1657428

Frydenvang, K., Verkade-Vreeker, M. C. A., Dohmen, F., Commandeur, J. N. M., Rafiq, M., Mirza, O., Jorgensen, F. S., & Geerke, D. P. (2019). Structural analysis of Cytochrome P450 BM3 mutant M11 in complex with dithiothreitol. *PLoS One*. *14*(5), e0217292. https://doi.org/10.1371/journal.pone.0217292

Ganesh, K., & Massague, J. (2021). Targeting metastatic cancer. *Nature Medicine*, *27*(1), 34–44. https://doi.org/10.1038/s41591-020-01195-4

Ghanadian, M., Ali, Z., Khan, I. A., Balachandran, P., Nikahd, M., Aghaei, M., Mirzaei, M., & Sajjadi, S. E. (2020). A new sesquiterpenoid from the shoots of Iranian Daphne mucronata Royle with selective inhibition of STAT3 and Smad3/4 cancer-related signaling pathways. *Daru*, *28*(1), 253–262. https://doi.org/10.1007/s40199-020-00336-x

Ghosh, D., Griswold, J., Erman, M., & Pangborn, W. (2010). X-ray structure of human aromatase reveals an androgen-specific active site. *The Journal of Steroid Biochemistry and Molecular Biology*, *118*(4-5), 197–202. https://doi.org/10.1016/j.jsbmb.2009.09.012

Glomb, T., Szymankiewicz, K., & Swiatek, P. (2018). Anti-cancer activity of derivatives of 1,3,4-oxadiazole. *Molecules*, *23*(12), 3361. https://doi.org/10.3390/molecules23123361

Harris, A. L. (2020). Development of cancer metabolism as a therapeutic target: New pathways, patient studies, stratification and combination therapy. *British Journal of Cancer*, *122*(1), 1–3. https://doi.org/10.1038/s41416-019-0666-4

Hoelder, S., Clarke, P. A., & Workman, P. (2012). Discovery of small molecule cancer drugs: Successes, challenges and opportunities. *Molecular Oncology*, *6*(2), 155–176. https://doi.org/10.1016/j.molonc.2012.02.004

Holohan, C., Van Schaeybroeck, S., Longley, D. B., & Johnston, P. G. (2013). Cancer drug resistance: An evolving paradigm. *Nature Reviews Cancer*, *13*(10), 714–726. https://doi.org/10.1038/nrc3599

Housman, G., Byler, S., Heerboth, S., Lapinska, K., Longacre, M., Snyder, N., & Sarkar, S. (2014). Drug resistance in cancer: An overview. *Cancers*, *6*(3), 1769–1792. https://doi.org/10.3390/cancers6031769

Jiang, Y. C., Feng, H., Lin, Y. C., & Guo, X. R. (2016). New strategies against drug resistance to herpes simplex virus. *International Journal of Oral Science*, *8*(1), 1–6. https://doi.org/10.1038/ijos.2016.3

Kaplancikli, Z. A., Yurttaş, L., Turan-Zitouni, G., Özdemir, A., Özic, R., & Ulusoylar-Yildirim, Ş. (2012). Synthesis, antimicrobial activity and cytotoxicity of some new carbazole derivatives. *Journal of Enzyme Inhibition and Medicinal Chemistry*, *27*(6), 868–874. https://doi.org/10.3109/14756366.2011.622273

Leary, M., Heerboth, S., Lapinska, K., & Sarkar, S. (2018). Sensitization of drug resistant cancer cells: A matter of combination therapy. *Cancers (Basel)*, *10*(12), 483. https://doi.org/10.3390/cancers10120483

Lipinski, C. A., Lombardo, F., Dominy, B. W., & Feeney, P. J. (1997). Experimental and computational approaches to estimate solubility and permeability in drug discovery and development settings. *Adv Drug Deliv Rev*, *23*(1-3), 3–25. https://doi.org/10.1016/S0169-409X(96)00423-1

Liu, Z., Fan, B., Zhao, J., Yang, B., & Zheng, X. (2023). Benzothiazole derivatives-based supramolecular assemblies as efficient corrosion inhibitors for copper in artificial seawater: Formation, interfacial release and protective mechanisms. *Corrosion Science*, *212*, 110957. https://doi.org/10.1016/j.corsci.2022.110957

Mamdani, H., Matosevic, S., Khalid, A. B., Durm, G., & Jalal, S. I. (2022). Immunotherapy in lung cancer: Current landscape and future directions. *Frontiers in Immunology*, *13*, 823618. https://doi.org/10.3389/fimmu.2022.823618

Markovic, A., Zivkovic, A., Atanasova, M., Doytchinova, I., Hofmann, B., George, S., Kretschmer, S., Rodl, C., Steinhilber, D., Stark, H., & Smelcerovic, A. (2023). Thiazole derivatives as dual inhibitors of deoxyribonuclease I and 5-lipoxygenase: A promising scaffold for the development of neuroprotective drugs. *Chemico-Biological Interactions*, *381*, 110542. https://doi.org/10.1016/j.cbi.2023.110542

Matore, B. W., Banjare, P., Guria, T., Roy, P. P., & Singh, J. (2022). Oxadiazole derivatives: Histone deacetylase inhibitors in anticancer therapy and drug discovery. *European Journal of Medicinal Chemistry Reports*, *5*, 100058. https://doi.org/10.1016/j.ejmcr.2022.100058

Nuha, D., Evren, A. E., Kapusiz, Ö., Gül, Ü. D., Gundogdu-Karaburun, N., Karaburun, A. Ç., & Berber, H. (2023). Design, synthesis, and antimicrobial activity of novel coumarin derivatives: An in-silico and in-vitro

study. *Journal of Molecular Structure*. *1272*, 134166. https://doi.org/10.1016/j.molstruc.2022.134166

Nuha, D., Evren, A. E., Yılmaz Cankılıç, M., & Yurttaş, L. (2021). Design and synthesis of novel 2,4,5-thiazole derivatives as 6-APA mimics and antimicrobial activity evaluation. *Phosphorus, Sulfur, and Silicon and the Related Elements*, *196*(10), 954–960. https://doi.org/10.1080/10426507.2021.1946537

Old, L. J., & Chen, Y. T. (1998). New paths in human cancer serology. *The Journal of Experimental Medicine*, *187*(8), 1163–1167. https://doi.org/10.1084/jem.187.8.1163

Osmaniye, D., Evren, A. E., Karaca, Ş., Özkay, Y., & Kaplancıklı, Z. A. (2023). Novel thiadiazol derivatives; design, synthesis, biological activity, molecular docking and molecular dynamics. *Journal of Molecular Structure*. *1272*, 134171. https://doi.org/10.1016/j.molstruc.2022.134171

Osmaniye, D., Levent, S., Karaduman, A. B., Ilgin, S., Ozkay, Y., & Kaplancikli, Z. A. (2018). Synthesis of new benzothiazole acylhydrazones as anticancer agents. *Molecules*, *23*(5), 1054. https://doi.org/10.3390/molecules23051054

Ozben, T. (2006). Mechanisms and strategies to overcome multiple drug resistance in cancer. *FEBS Letters*, *580*(12), 2903–2909. https://doi.org/10.1016/j.febslet.2006.02.020

Ozdemir, A., Sever, B., Altintop, M. D., Temel, H. E., Atli, O., Baysal, M., & Demirci, F. (2017). Synthesis and evaluation of new oxadiazole, thiadiazole, and triazole derivatives as potential anticancer agents targeting MMP-9. *Molecules*, *22*(7), 1109. https://doi.org/10.3390/molecules22071109

Pan, M. H., Ghai, G., & Ho, C. T. (2008). Food bioactives, apoptosis, and cancer. *Molecular Nutrition & Food Research*, *52*(1), 43–52. https://doi.org/10.1002/mnfr.200700380

Raguz, S., & Yague, E. (2008). Resistance to chemotherapy: New treatments and novel insights into an old problem. *British Journal of Cancer*, *99*(3), 387–391. https://doi.org/10.1038/sj.bjc.6604510

Rashid, M., Husain, A., Mishra, R., Karim, S., Khan, S., Ahmad, M., Al-Wabel, N., Husain, A., Ahmad, A., & Khan, S. A. (2019). Design and synthesis of benzimidazoles containing substituted oxadiazole, thiadiazole and triazolo-thiadiazines as a source of new anticancer agents. *Arabian Journal of Chemistry*. *12*(8), 3202–3224. https://doi.org/10.1016/j.arabjc.2015.08.019

Riggio, A. I., Varley, K. E., & Welm, A. L. (2021). The lingering mysteries of metastatic recurrence in breast cancer. *British Journal of Cancer*, *124*(1), 13–26. https://doi.org/10.1038/s41416-020-01161-4

Ross, J. S., Wang, K., Gay, L., Al-Rohil, R., Rand, J. V., Jones, D. M., Lee, H. J., Sheehan, C. E., Otto, G. A., Palmer, G., Yelensky, R., Lipson, D., Morosini, D., Hawryluk, M., Catenacci, D. V., Miller, V. A., Churi, C., Ali, S., & Stephens, P. J. (2014). New routes to targeted therapy of intrahepatic cholangiocarcinomas revealed by next-generation sequencing. *The Oncologist*, *19*(3), 235–242. https://doi.org/10.1634/theoncologist.2013-0352

Sağlık, B. N., Şen, A. M., Evren, A. E., Çevik, U. A., Osmaniye, D., Kaya Çavuşoğlu, B., Levent, S., Karaduman, A. B., Özkay, Y., & Kaplancıklı, Z. A. (2020). Synthesis, investigation of biological effects and in silico studies of new benzimidazole derivatives as aromatase inhibitors. *Zeitschrift Fur Naturforschung. C, Journal of Biosciences*, *75*(9–10), 353–362. https://doi.org/10.1515/znc-2020-0104

Sahin, Z., Ertas, M., Berk, B., Biltekin, S. N., Yurttas, L., & Demirayak, S. (2018). Studies on non-steroidal inhibitors of aromatase enzyme; 4-(aryl/heteroaryl)-2-(pyrimidin-2-yl)thiazole derivatives. *Bioorganic & Medicinal Chemistry*, *26*(8), 1986–1995. https://doi.org/10.1016/j.bmc.2018.02.048

Schrödinger. (2020a). *Schrödinger Release 2020-3, Desmond*. Schrödinger, LLC.

Schrödinger. (2020b). *Schrödinger Release 2020-3, Glide*. Schrödinger, LLC.

Schrödinger. (2020c). *Schrödinger Release 2020-3: LigPrep 2020*. Schrödinger, LLC.

Schrödinger. (2020d). *Schrödinger Release 2020-3*, Maestro. Schrödinger, LLC.

Subramaniam, S., Selvaduray, K. R., & Radhakrishnan, A. K. (2019). Bioactive compounds: Natural defense against cancer? *Biomolecules*, *9*(12), 758. https://doi.org/10.3390/biom9120758

Sun, G., Rong, D., Li, Z., Sun, G., Wu, F., Li, X., Cao, H., Cheng, Y., Tang, W., & Sun, Y. (2021). Role of small molecule targeted compounds in cancer: Progress, opportunities, and challenges. *Frontiers in Cell and Developmental Biology*, *9*, 694363. https://doi.org/10.3389/fcell.2021.694363

Suvannang, N., Nantasenamat, C., Isarankura-Na-Ayudhya, C., & Prachayasittikul, V. (2011). Molecular docking of aromatase inhibitors. *Molecules*, *16*(5), 3597–3617. https://doi.org/10.3390/molecules16053597

Turan Yucel, N., Evren, A. E., Kandemir, U., & Can, O. D. (2022). Antidepressant-like effect of tofisopam in mice: A behavioural, molecular docking and MD simulation study. *Journal of Psychopharmacology (Oxford, England)*, *36*(7), 819–835. https://doi.org/10.1177/02698811221095528

Vaidya, F. U., Sufiyan Chhipa, A., Mishra, V., Gupta, V. K., Rawat, S. G., Kumar, A., & Pathak, C. (2022). Molecular and cellular paradigms of multidrug resistance in cancer. *Cancer Rep (Hoboken)*, *5*(12), e1291.

Venkatesham, P., Schols, D., Persoons, L., Claes, S., Sangolkar, A. A., Chedupaka, R., & Vedula, R. R. (2023). Synthesis of novel thioalkylated triazolothiazoles and their promising in-vitro antiviral activity. *Journal of Molecular Structure*. *1286*, 135573. https://doi.org/10.1016/j.molstruc.2023.135573

Wijdeven, R. H., Pang, B., Assaraf, Y. G., & Neefjes, J. (2016). Old drugs, novel ways out: Drug resistance toward cytotoxic chemotherapeutics. *Drug Resistance Updates: Reviews and Commentaries in Antimicrobial and Anticancer Chemotherapy*, *28*, 65–81. https://doi.org/10.1016/j.drup.2016.07.001

Xu, T., Tian, W., Zhang, Q., Liu, J., Liu, Z., Jin, J., Guo, Y., & Bai, L. P. (2021). Novel 1,3,4-thiadiazole/oxadiazole-linked honokiol derivatives suppress cancer via inducing PI3K/Akt/mTOR-dependent autophagy. *Bioorganic Chemistry*, *115*, 105257. https://doi.org/10.1016/j.bioorg.2021.105257

Yavari, I., Sayyed-Alangi, S. Z., Hajinasiri, R., & Sajjadi-Ghotbabadi, H. (2008). A one-pot synthesis of functionalized ethyl 1,3-thiazole-5-carboxylates from thioamides or thioureas and 2-chloro-1,3-dicarbonyl compounds in an ionic liquid. *Monatshefte Für Chemie - Chemical Monthly*, *140*(2), 209–211. https://doi.org/10.1007/s00706-008-0900-x

Yersal, O., & Barutca, S. (2014). Biological subtypes of breast cancer: Prognostic and therapeutic implications. *World Journal of Clinical Oncology*, *5*(3), 412–424. https://doi.org/10.5306/wjco.v5.i3.412

Yin, L., Duan, J. J., Bian, X. W., & Yu, S. C. (2020). Triple-negative breast cancer molecular subtyping and treatment progress. *Breast Cancer Research: BCR*, *22*(1), 61. https://doi.org/10.1186/s13058-020-01296-5

Zhang, J., Wang, X., Yang, J., Guo, L., Wang, X., Song, B., Dong, W., & Wang, W. (2020). Novel diosgenin derivatives containing 1,3,4-oxadiazole/thiadiazole moieties as potential antitumor agents: Design, synthesis and cytotoxic evaluation. *European Journal of Medicinal Chemistry*, *186*, 111897. https://doi.org/10.1016/j.ejmech.2019.111897

Zhong, L., Li, Y., Xiong, L., Wang, W., Wu, M., Yuan, T., Yang, W., Tian, C., Miao, Z., Wang, T., & Yang, S. (2021). Small molecules in targeted cancer therapy: Advances, challenges, and future perspectives. *Signal Transduction and Targeted Therapy*, *6*(1), 201.